Investigation of radiation-dose-induced changes in organic light-atom crystals by accurate *d*-spacing measurements†

Ralf Müller,[a]* Edgar Weckert,[b] Johannes Zellner[a] and Michael Drakopoulos[c]

[a]Institut für Kristallographie, RWTH-Aachen, Germany, [b]HASYLAB, DESY, Hamburg, Germany, and [c]ESRF, Grenoble, France. E-mail: ralf@deres-mueller.de

Changes in *d*-spacing have been measured for organic compounds as a function of temperature, wavelength and primary beam intensity using intense synchrotron radiation. The *d*-spacings of organic and protein crystals were found to increase irreversibly as a function of radiation dose. The activation energy of this thermally activated process was estimated. No evidence for a significant temperature increase of the sample due to exposure to intense X-ray beams could be found experimentally for flux densities up to 4×10^{12} photons s^{-1} mm^{-2}.

Keywords: radiation damage; *d*-spacing measurements.

1. Introduction

Protein crystals, and also other organic compounds, are known to suffer seriously from radiation damage under exposure to intense X-ray beams. Cooling the crystals to low temperatures in general slows down radiation damage (Garman & Schneider, 1997) most probably by lowering the rate of thermally activated processes. For very high flux densities, heating of the crystals might also occur. Following the arguments given by Helliwell (1992), even crystals of low-*Z* elements absorb a considerable amount of the energy of the incident beam. It is assumed that a large fraction of the absorbed energy is converted to heat. If we assume a heat capacity the same as ice at 100 K (0.838 J g^{-1} K^{-1}) and adiabatic conditions for the crystal except of the incident photon beam, a 0.3 mm-size cube-shaped crystal of a low-*Z* element compound will heat up at a rate of 0.62 K s^{-1} in a 4×10^{12} photons s^{-1} mm^{-2} beam of wavelength $\lambda = 1.0$ Å. The heating rate can be four to five times higher if a 10^{14} photons s^{-1} mm^{-2} beam hits, for example, a sample of size 50 µm. These are conditions comparable with high-brilliance focused undulator beamlines at third-generation synchrotron radiation sources. In a real experiment the actual sample temperature depends also on the cooling rate. In the case of a gas-flow cryocooler it is governed mainly by heat transfer from the crystal surface to the cooling gas and the heat conductivity inside the sample which in the general case consists of a crystal embedded in vitreous ice. A recent and more detailed study applying finite-element-based heat conductivity calculations and taking into account proper interface heat-transfer coefficients predicts a relatively fast sample temperature change of about 4 K for a 0.1 mm-size crystal hit by a 0.05 mm beam of 10^{15} photons s^{-1} mm^{-2} flux density (Nicholson *et al.*, 2001).

Accurate temperature measurement of small crystal samples, *e.g.* with a thermocouple, is difficult. However, the thermal expansion can be determined by accurate *d*-spacing measurements. During normal intensity data collections from protein crystals using area detectors it

has been observed (Burmeister, 2000; Ravelli & McSweeny, 2000; Weik *et al.*, 2001) that *d*-spacings also change as a function of the absorbed radiation dose. Therefore, the effects of radiation damage and thermal expansion have to be separated in a suitable manner.

Although the primary interest of these investigations is in macromolecular structural crystallography to obtain preliminary insights into the feasibility of the envisaged investigation, organic light-atom small-molecule compounds were used as model compounds for protein crystals. They show approximately the same mass absorption coefficient and chemical composition but they lack the highly mobile and disordered solvent regions that are present in protein crystals. In a first experiment the thermal expansion of the compounds was determined using a low-intensity beam. In the following experiments the irreversible changes in *d*-spacing were investigated in detail at high photon flux densities. Using the information of the previous experiments, investigations about a possible temperature rise due to an increased flux density were carried out. All successive experiments concentrated on the radiation-damage-induced change in *d*-spacing which was investigated as a function of radiation energy and temperature. During the course of all experiments, rocking curves were measured that allowed an almost continuous monitoring of the sample's mosaicity.

2. Experimental

2.1. Apparatus and samples

The experiments were carried out at ESRF beamline ID22. The radiation source was a 1.65 m-long 38-pole high-β undulator. The beam was not focused. An Si(111) cryogenic-cooled double-crystal monochromator was used providing a bandpass of approximately 1.4×10^{-4} over the applied wavelength range 0.45–1.5 Å. For the lower energies a flat horizontally deflecting mirror was used to reduce the contributions of higher harmonics. The flux was measured with a calibrated pin diode. The actual flux density for each experiment is given below in each individual case. The rocking curves were recorded by a high-resolution Ψ six-circle diffractometer (Weckert & Hümmer, 1997) using a point detector with a high-count-rate-capable plastic scintillator (Zellner, 1996). The smallest possible step width for the ω circle used for *d*-spacing measurements is 5×10^{-5} degrees. Despite the high-count-rate detector ($I_{max} > 10^7$ counts s^{-1}), strong absorbers had to be used in front of the detector. For all *d*-spacing measurements, reflection profiles were recorded and stored. The angular position of the peaks θ_{max} on each side of the primary beam (Fig. 1) was calculated from

$$\theta_{max} = \sum_i \omega I_i^5 / \sum_i I_i^5. \tag{1}$$

The sum runs over all step points with intensity $I_i > I_{max}/2$. The exponent 5 in (1) ensures that the region around the intensity maximum receives the most weight in determining the peak position. The crystals of the investigated low-*Z* compounds [L-asparagine monohydrate (Ramanadham *et al.*, 1972) and sucrose (Hynes & Le Page, 1991)] were between 400 and 600 µm in size in all three dimensions. For the experiments reported here, the beam size was always adjusted such that the whole crystal was illuminated. Crystals were cooled with a cryojet cooler. The temperatures given correspond to the reading of this device.

2.2. Measurement techniques

For good quality crystals, as in the case of the small-molecule samples studied (mosaicity: FWHM $\simeq 0.01°$), a change in *d*-spacing can be measured from the corresponding shift in Bragg angle

deduced directly from the maxima of the rocking curve. In order to avoid zero point and setting errors the Bragg angles were determined by the Bond method (Fig. 1) (Bond, 1960).

The Bond method becomes less accurate if the crystal's mosaicity is increased, *e.g.* owing to bad crystal quality or to increasing radiation damage. For this reason, *d*-spacing measured using the Bond method at relatively high integrated radiation doses in general cannot be used for quantitative evaluations of the *d*-spacing. The same holds for frozen protein crystals since their mosaicity is in general also too high. For highly mosaic crystals the use of an analyser crystal and application of a scan parallel to the direction of the reciprocal lattice vector ($\omega/2\theta$ scan) of the reflection to be investigated will still provide very accurate *d*-values (Fig. 2).

The experimental effort for this method is somewhat higher; however, it is in principle much faster since only one scan has to be carried out instead of the two using the Bond method. The analyser crystal technique also avoids long time-consuming driving distances for the diffractometer. For the experiment described, the Bond method was applied for the investigation of organic small-molecule compounds. The experiments using shock-frozen protein crystals were carried out using the analyser crystal technique.

2.3. Determination of the thermal expansion

Using the variation of *d*-spacing to derive temperature information requires an accurate knowledge of the thermal expansion. A low flux was used to determine the thermal expansion by the Bond method of L-asparagine monohydrate (Fig. 3) and sucrose. Owing to the available beam time the measurement was restricted to one direction only, therefore, a full thermal expansion tensor was not obtained. For L-asparagine monohydrate the (147)-reflection was chosen, which is a
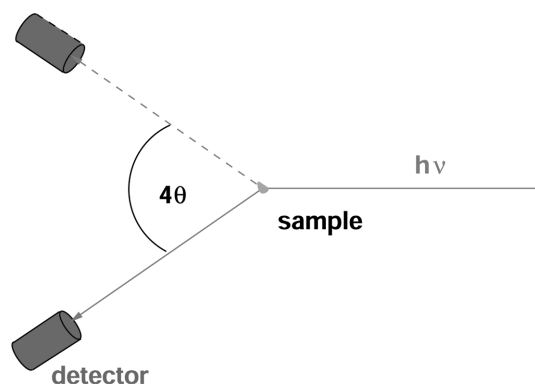
compromise for both a relatively large $|F(\mathbf{h})|$ and a large θ value which is necessary for precise *d*-spacing measurements.

2.4. Change of *d*-spacing as function of radiation dose

A crystal of L-asparagine monohydrate was continuously exposed for several 15–20 min-long periods to a flux density of about 4×10^{12} photons s^{-1} mm^{-2} at 100 K for $\lambda = 1$ Å. During the exposure the *d*-spacing of the (147)-reflection was monitored. In between these exposure periods the shutter was closed. For the third exposure period the beam was attenuated by a 300 µm Al foil (transmission: 0.356). After about 120 min the temperature was raised within 35 min to 270 K and a last exposure period monitoring the *d*-spacing was carried out.

2.5. Investigation of beam heating

In order to investigate possible effects of sample heating by the beam the *d*-spacing was determined several times for a given temperature at low flux. At a given time, denoted by $t = 0$, the absorber was removed and the full beam was incident on the crystal with the *d*-spacing monitored continuously for about 30–40 min in order to obtain d*d*/d*t* with sufficient accuracy.

2.6. Reflection profiles

Rocking-curve profiles were obtained by the ω-scan technique with a step width of $\Delta\omega = 5 \times 10^{-4}$ degrees and 0.1 s measurement time per step using a point detector. The detector opening was about 0.5° in order to integrate over the whole diffracted beam.

2.7. Temperature dependence

The temperature dependence of d*d*/d*t* was investigated in a temperature range from 100 K to 220 K at $\lambda = 1$ Å. For this investigation the *d*-spacing was monitored under continuous crystal illumination at each given temperature. The total exposure time for one temperature data point was about 30–45 min in order to determine d*d*/d*t* with sufficient accuracy as shown *e.g.* in Fig. 5 for $t > 0$. The shutter was kept closed during the time the temperature was changed. Two different crystals of L-asparagine monohydrate were necessary to obtain all data.

Figure 1
The scattering angle is measured with high precision at both sides of the primary beam using the same scan rotation sense. Possible zero-point offsets and setting errors of the crystal cancel hereby.
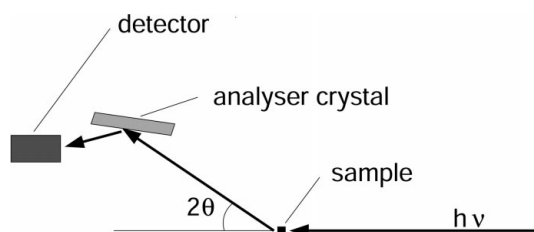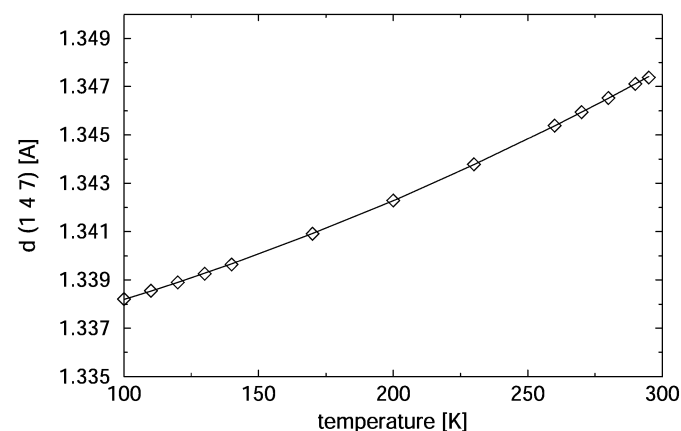

Figure 2
Schematic view of a simple analyser crystal setup. In the case of higher mosaicity, *d*-spacing changes are more accurately determined by using an analyser crystal and scans parallel to the reciprocal lattice vectors ($\omega/2\theta$-scan).

Figure 3
Temperature dependence of the *d*-value of reflection (147) for L-asparagine monohydrate. The solid line corresponds to a least-squares fit of $d = (1.33542 + 2.1 \times 10^{-5}\, T + 6.7 \times 10^{-8}\, T^2)$ Å.

2.8. Energy dependence

The energy dependence of the change in lattice spacing dd/dt was studied in the wavelength range 0.45–1.5 Å. The experiments were carried out at a constant temperature of 100 K. Otherwise the procedure was similar to that used to study the temperature dependence. Five different crystals of L-asparagine monohydrate were necessary to cover the envisaged energy range.

3. Results

3.1. Thermal expansion

Fig. 3 shows the d-spacing for the (147) reflection of L-asparagine monohydrate from 100 K to 300 K. There is a slight deviation from a purely linear dependency of $d_{(147)}$ on temperature. For this reason a least-squares fit of a parabola was applied resulting in $d_{(147)} = [1.33542\,(6) + 2.10\,(6) \times 10^{-5}\,T + 6.7\,(2) \times 10^{-8}\,T^2]$ Å. This temperature dependence was used for all subsequent evaluations.

3.2. Change of *d*-spacing as a function of radiation dose

Fig. 4 shows the change of the d-spacing of the (147) reflection of L-asparagine monohydrate for a flux density of $\sim 4 \times 10^{12}$ photons s^{-1} mm^{-2} and 1.38×10^{12} photons s^{-1} mm^{-2} labelled as 'full beam' and '$\sim 1/3$', respectively. The d-values determined after each 'shutter closed' period are almost the same as the last value obtained during the previous continuous exposure period. This indicates an irreversible increase of the d-spacings with radiation dose for this small-molecule compound as has been found by others for protein crystals (Weik *et al.*, 2001; Burmeister, 2000; Ravelli & McSweeney, 2000). The increase is, to a very good approximation, linear with a correlation coefficient > 99.7% for all segments shown in Fig. 4 and for the dose rates applied. The slopes dd/dt for the three different measurement series at full beam and 100 K were reproducible within 1%. If the beam was attenuated by a 300 μm Al foil (transmission: 0.346), the slope dd/dt decreased to 0.344 times the value of the full beam. This indicates, at least for these conditions, a linear dependence of dd/dt from the flux density. The FWHM of the reflection was 0.013° at the beginning of the experiment; after 120 min and a dose of about 10 MGy it was 0.019°. In addition, the reflections started to show large 'wings'. Therefore, the damage was more severe than the
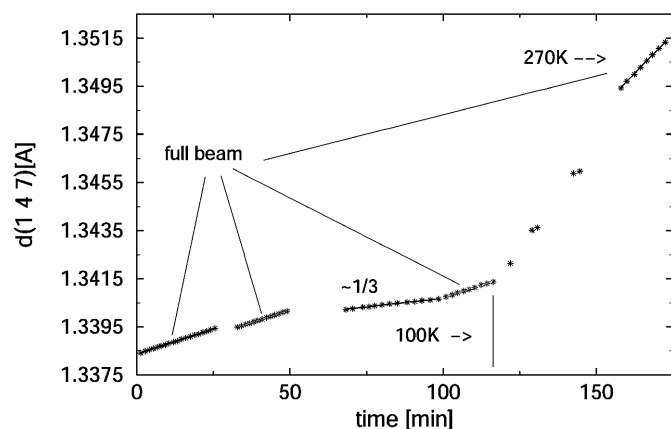
change in FWHM indicates. The theoretical minimal FWHM of the experimental setup at the (147) Bragg angle is about 0.0034°. The FWHM approached 0.1° at the end of the experiment when the crystal was almost destroyed.

A comparison of the data points at 100 K and 270 K in Fig. 4 shows that dd/dt depends significantly on the temperature for a given flux.

The conclusions of this experiment are (i) there is a linear and irreversible change in lattice parameters with radiation dose; (ii) at the dose rates tested, dd/dt is approximately linear with the flux density; (iii) as expected, dd/dt depends strongly on the temperature; (iv) a temperature change due to the absorbed energy must be small. From these results there is further strong evidence (v) that the radiation damage of the sample is directly correlated to the irreversible change in lattice spacing. These assumptions were used for all of the following investigations.

3.3. Investigation of beam heating

The mean d-value of the measurements at low flux is indicated by the horizontal line in Fig. 5. At the time indicated by $t = 0$ s the full beam was switched on by removing a beam attenuator, and the
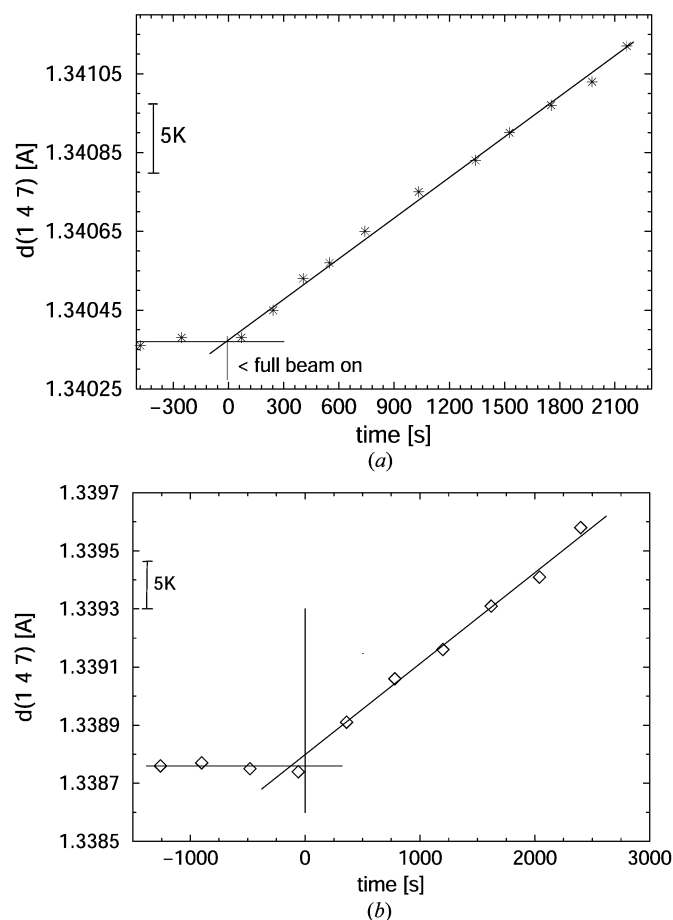

(a)

(b)

Figure 5
Change in d-spacing of reflection (147) of L-asparagine monohydrate with low and high photon flux for two different crystals and temperatures. No significant jump in temperature can be observed. The d-spacing change calculated based on the results shown in Fig. 3 for a 5 K temperature difference is indicated. (*a*) Primary beam flux was in the 10^9 photons s^{-1} mm^{-2} range to the left and 3×10^{12} photons s^{-1} mm^{-2} to the right of the line at $t = 0$ s, $\lambda = 1$ Å, $T = 140$ K. (*b*) Primary beam flux was 8.6×10^7 photons s^{-1} mm^{-2} to the left and 2.1×10^{12} photons s^{-1} mm^{-2} to the right of the line at $t = 0$ s, $\lambda = 0.8$ Å, $T = 100$ K.

Figure 4
Change of d-spacing of reflection (147) as a function of time/dose of L-asparagine monohydrate, $T = 100$ K, $\lambda = 1.0$ Å, at different beam intensities. Starting at full beam ($\sim 4 \times 10^{12}$ photons s^{-1} mm^{-2}) for the measurement points labelled by '1/3', the beam was attenuated by a 300 μm Al foil. The crystal was continuously illuminated except during the gaps in the diagram. The temperature was set to 270 K for the experiments after $t = 150$ min. See main text for further information.

evolution of the *d*-spacing with time is shown. The increase in *d* was least-squares fitted with a line. From a linear back extrapolation the *d*-spacing shortly after *t* = 0 s can be estimated. It is possible to estimate the accuracy of this back extrapolation from the standard deviations of the fitted parameters. The small increase at *t* = 0 s that can be seen in the lower graph of Fig. 5 at *t* = 0 corresponds to about 1.9 K which is about two times the standard deviation for this quantity in that particular case. The flux densities applied are given in the figure captions as well as the temperature at which the experiments were carried out.

3.4. Reflection profiles

Radiation damage has also significant influence on the reflection profiles and peak intensity. Owing to the loss of peak intensity and the increase in width, the signal-to-noise ratio of a damaged crystal becomes worse. As in the example shown in Fig. 6, the peak intensity decreases by a factor of about two during 200 min of exposure at a flux density of about $\sim 10^{12}$ photons s^{-1} mm^{-2}, and the FWHM increases from $0.0075°$ to $0.015°$. However, from the shape of the profile it is obvious that the crystal has suffered more severe damage than is indicated by the increase in the profile's FWHM since the reflection profile developed already a quite extended 'tail' at the right-hand side of the main peak (Fig. 6). At the same time the integrated intensity has changed by less than 2%. The influence on $I/\sigma(I)$ in this case is not dramatic since it is a strong reflection of a small-molecule compound; however, the situation is certainly worse for reflections with smaller intensities as they are more common in protein crystals. After 360 min of exposure even this small-molecule crystal was effectively destroyed, showing no significant reflections in the higher-resolution range.

3.5. Temperature dependence

Thermally activated processes are normally described by an Arrhenius-type expression. In the case of the rate of the increase of the lattice spacing this is

$$\partial d/\partial t = k \exp(-E_a/k_{\mathrm{B}}T), \qquad (2)$$

with scaling constant k, activation energy E_a and Boltzmann constant k_{B}. Following the results shown in Fig. 4, the constant k is approximately proportional to the flux density. In order to obtain at least a rough estimate of the activation energy and maybe also of the nature of the underlying rate-controlling process, dd/dt was measured for different temperatures. The results of some of these measurements are shown in Fig. 7. From these experiments an activation energy
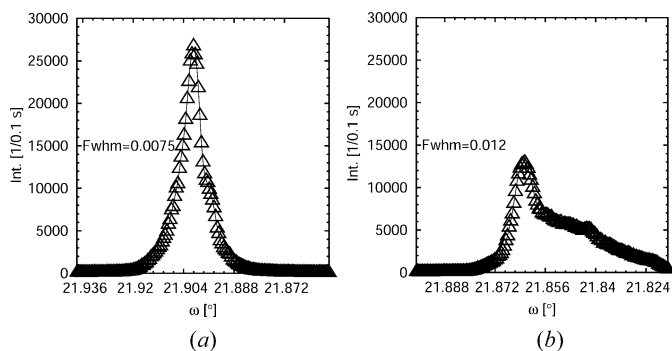
$\{-\partial \ln[(\mathrm{d}d/\mathrm{d}t)/k]/\partial(1/T)\}/k_{\mathrm{B}} = E_a$ of about 10 (1) meV was deduced. The accuracy of this value is limited, but it should indicate the right order of magnitude. Owing to the fast increase in mosaicity that caused problems in the determination of an accurate *d*-spacing by the Bond method, especially at temperatures significantly above 100 K, two crystals had to be used in order to collect the data for the determination of E_a. The slopes of the individual Arrhenius plots were more or less of the same order of magnitude; however, slightly but significantly different values of the constant k in (2) were observed. The exact reason for this behaviour is not known. A possible reason could be the slightly different size of the crystal samples.

3.6. Energy dependence

In the upper part of Fig. 8 the results for the energy dependence of dd/dt at a temperature of 100 K is shown. The flux density for different wavelengths during these experiments ranged from 5.8×10^{10} photons s^{-1} mm^{-2} at low energies to 2.1×10^{12} photons s^{-1} mm^{-2} at $\lambda = 0.8$ Å and to 1.04×10^{12} photons s^{-1} mm^{-2} at $\lambda = 0.45$ Å. Under the assumption that dd/dt is proportional to the flux density, which is based on the results shown in Fig. 4, the dd/dt values shown in Fig. 8 were all scaled to a flux density of 10^{11} photons s^{-1} mm^{-2}.

4. Discussion

Beam heating. The results shown in Fig. 5 indicate that a possible temperature increase must be smaller than about 1–2 K. In summary, from a larger number of experiments, no significant ($\Delta T > 2$ K) change in temperature for a number of L-asparagine monohydrate and sucrose crystals could be found. It seems that the absorbed heat is carried away for the applied fluxes in samples like these. The applied flux densities of several 10^{12} photons s^{-1} mm^{-2} are smaller than at focused undulator beamlines of third-generation sources. At the same time, typical crystal sizes at such beamlines are considerably smaller than those used for the present experiments which were ~ 500 µm in all dimensions. Therefore, a smaller fraction of the radiation will be absorbed, the surface to volume ratio is larger, and a certain temperature change in the middle of the crystal will result in a larger gradient dT/dx leading very likely to more efficient cooling.
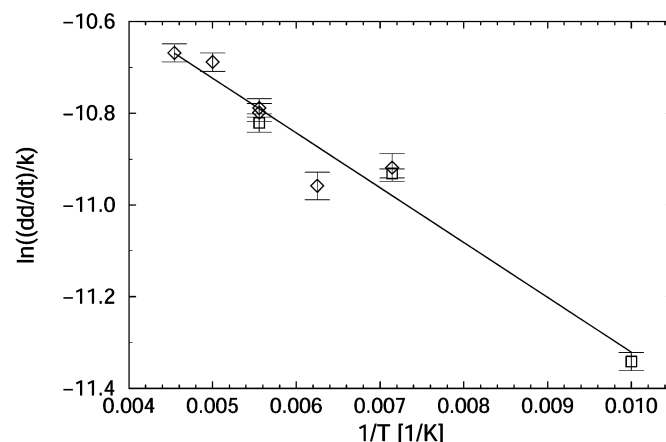

Figure 6
Reflection profile of (147) of L-asparagine monohydrate at the beginning (left) and after 200 min exposure (right); $\lambda = 1$ Å, primary flux $\sim 10^{12}$ photons s^{-1} mm^{-2}, T = 160–200 K.

Figure 7
Arrhenius plot for the rate of *d*-spacing increase in L-asparagine monohydrate crystals at $\lambda = 1.0$ Å. Different crystals showed more or less the same slopes but often a different constant k (equation 2). For this figure, the constant k of both crystals was scaled such that all values fell approximately on a single line. The individual slopes were −120 (squares) and −115.5 (diamonds). The slope of the least-squares line shown is −119.4 (10.3).

Since the whole situation seems to be quite complex it is not straightforward to extrapolate from the presented results to focused beamlines and smaller crystals. For this reason, further experiments under theses conditions are necessary.

Temperature dependence. The primary inelastic interaction process of X-rays with atoms is photoabsorption. Only at higher energies (*e.g.* $\lambda = 0.45$ Å) does photoabsorption become small and comparable in cross section with inelastic Compton scattering. During a photo-absorption event almost the whole photon energy is transferred to the crystal since the mean free path length for the primary photo-electron as well as for the secondary Auger electrons, that are created if inner shell holes decay, is extremely short in dense matter. In contrast, the energy transfer for an inelastic Compton event is small compared with the photoeffect; however, the scattered photon is lost for the elastic scattering process. These primary radiation-damage processes are certainly independent of temperature.

For each photoabsorption event a number of ionized atoms, free radicals and broken bonds are created. Since these species are quite reactive, secondary processes take place which are assumed to have a thermally activated rate-controlling process because otherwise prolonged crystal lifetimes at lower temperatures could not be explained. These secondary processes are probably the main reason for the increase in *d*-spacing and the destruction of the crystal.

For the determination of the activation energy it was assumed that the rate-controlling process stays the same over the investigated temperature range. The determined activation energy of 10 meV seems to be too small for diffusion processes in dense matter. Just for comparison without any possible correlation to radiation damage, this activation energy is in the range of that of phonons. However, the local density around an atom that has experienced photoabsorption, meaning the release of about 10 keV energy or more in a relatively

small volume determined by the mean free path length of the ejected photoelectron, might be different from that of undisturbed material. Even if an estimate of the activation energy is now available it will probably be hard to trace down the corresponding process to a molecular or atomic level.

The measurements shown in Fig. 4 indicate that no significant changes take place at low temperatures on a time scale of several tens of minutes during the time the beam is switched off after a longer time of continuous exposure to an intense beam. Otherwise a larger difference in *d*-spacing between the last data point of an exposure series and the first one of the next series should be observed. This result and the observation of the very small activation energy make it unlikely that diffusion of reaction partners over larger distances is the rate-controlling process for radiation damage at low temperatures. The small activation energy might belong to the local atomic relaxation processes that will occur around atoms where primary photoelectrons or secondary Auger electrons were scattered inelas-tically. The energy transferred during such a process can be estimated to be in the 40 eV range (Perkins *et al.*, 1991), sufficient for a number of outer-shell ionizations or atom displacements. This hypothesis leads to the following time scales for radiation-damage processes for crystals at low temperatures: (i) The photoionization and Compton scattering process taking place on a time scale $\simeq 1$ as. (ii) Auger or fluorescence decay of the excited atoms will occur in ~ 1–10 fs. (iii) The next time scale is the thermalization of photo and Auger electrons which will still be extremely fast. (iv) The question now is, at what time scale do displaced or excited atoms or radicals relax or react with the immediate neighbours? It is certainly faster than the time resolution of the presented experiments. For a proper answer, further experiments appear to be necessary. (v) If the temperature is high enough for diffusion there will certainly be a slow process distributing the reaction products created during radiation impact over the crystal. It is also questionable how far this hypothetic scenario applies to protein crystals as well which are in general less dense than the investigated small-molecule compounds.

Energy dependence. The question whether there is an optimum radiation energy for crystallographic intensity data collections in the presence of significant radiation damage has already been discussed (*e.g.* Arndt, 1984; Gonzalez *et al.*, 1994). The integrated intensity in the kinematical limit is given by

$$I(h) = I_0 r_0^2 \left(\lambda^3 / \sin 2\theta \right) P |F(h)|^2 \left(V_{cr} / V_{uc}^2 \right) \exp(-\mu t), \qquad (3)$$

where I_0 is the incident flux density, $r_0 = 2.81 \times 10^{-5}$ Å is the classical electron radius, P is the polarization factor, V_{cr} is the volume of the crystal, V_{uc} is the volume of the unit cell and t is the path length of the beam inside the crystal. All other quantities have their usual mean-ings.

Neglecting polarization effects, the effective wavelength depen-dence is given by the Lorentz factor which gives a λ^2 dependence at low resolution. At high resolution ($\simeq 0.8$ Å) the dependence is about $\lambda^{2.5}$. For the following we concentrate on low-resolution reflections and use as a measure for the integrated kinematical intensity $Ik \propto \lambda^2 \exp(-\mu t)$. The absorption coefficient is approximately proportional to λ^3 and the absorbed energy proportional to $1/\lambda$ giving an effective λ^2 dependence as well. This rough assumption can be improved by calculating the absorption accurately from the known tabulated cross sections. For the discussion of radiation decay the cross section for the energy transfer is important and not the number of inelastic scattering events. The energy transfer ratio is very large for photoabsorption and relatively small for Compton scattered photons. For all following estimates, inelastic scattering cross sections
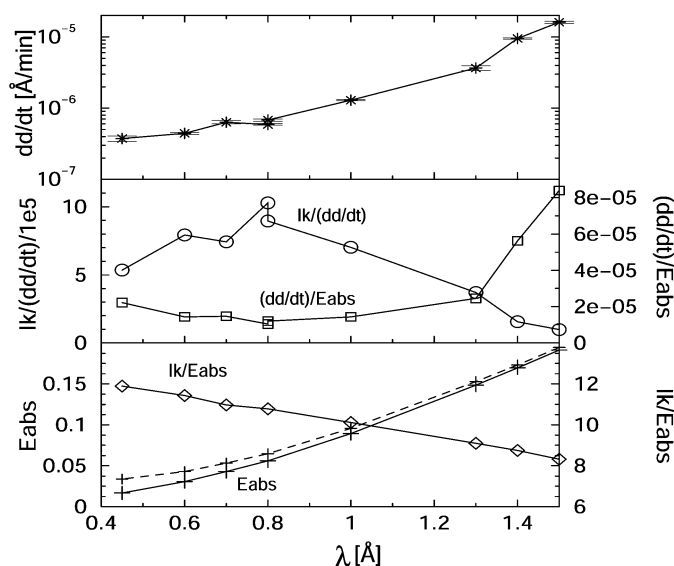

Figure 8
Top: rate of *d*-spacing change d*d*/d*t* normalized to a flux of 10^{11} photons s^{-1} mm^{-2} as a function of wavelength. Middle: integrated diffracted reflection intensity *Ik* normalized to the experimental d*d*/d*t* values and the same values normalized by the absorbed energy E_{abs}. The numbers are in arbitrary units. Bottom: total energy of the inelastic scattered photons (dashed), total transferred energy (solid) labelled by 'E_{abs}' and integrated diffracted reflection intensity normalized to the energy transfer in arbitrary units. The two data points at 0.8 Å have been measured from different crystals giving an indication of the reproducibility of the experimental data between different crystals of the same compound, which was L-asparagine monohydrate in this case. For all calculations a crystal thickness of 0.3 mm was assumed.

were taken from the EPDL97 database (Cullen *et al.*, 1997) which also contains cross sections for the energy transfer. In Fig. 8 (top) the experimentally determined values of dd/dt as a measure for the radiation decay are shown as a function of wavelength. For the following discussion, as a measure of the absorbed energy, $E_{abs} \propto [1 - \exp(-\mu' t)]/\lambda$ will be used; here μ' is derived from the energy-transfer inelastic cross sections. In Fig. 8 (bottom) the energy of all inelastic scattered photons is compared with the energy transferred. Differences occur mainly at higher energies where the Compton cross section is comparable to the photoabsorption cross section. The ratio Ik/E_{abs} in this graph shows only a small variation over the whole energy range which is consistent with earlier findings (Arndt, 1984). There is, however, an indication that higher energies are more favourable. One would expect that dd/dt is proportional to the absorbed energy E_{abs}, meaning that $(dd/dt)/E_{abs} = $ a constant. This is almost true for wavelengths below 1.3 Å as can be seen from Fig. 8 (middle). However, there is a significant deviation at lower energies. In the same graph $Ik/(dd/dt)$ is shown indicating that the optimum energy range is between 0.6 and 1.0 Å. Above 1 Å radiation damage increases and below 0.6 Å the diffracted integral intensity decreases faster than radiation damage.

These results are, of course, only a guideline since the investigated compound was of light elements only. If heavier elements are present the optimum wavelength will very likely shift to higher energies.

First application to protein crystals. Also for protein crystals [tetragonal hen egg-white lysozyme (Blake *et al.*, 1965)] a linear increase of the d-spacing with dose has been found during first experiments (Müller *et al.*, 2002), consistent with other experiments (Burmeister, 2000). With a flux density of $\sim 10^{12}$ photons s^{-1} mm^{-2} a relative change in d-spacing of $(dd/dt)/d = 2.61 \times 10^{-4}$ min and $(dd/dt)/d = 2.32 \times 10^{-5}$ min at $T = 300$ K and $T = 100$ K, respectively, was determined. These experiments were carried out using the analyser crystal technique. At 100 K the damage rate is about ten times smaller compared with at 300 K. This is certainly due to the reduced mobility of reaction products in the shock-frozen crystal compared with the room-temperature state with large highly mobile solvent regions. Compared with L-asparagine monohydrate the damage rate at 100 K is considerably higher. This might be explained by the large disordered solvent regions which very likely enable a larger mobility of radicals and ions even at low temperatures.

5. Conclusion

Some of the conclusions drawn in this investigation are based on the assumption that the change in lattice spacing is a suitable metric for radiation damage. For this purpose two experimental requirements have to be satisfied from our experience. (i) The Bond method works well only as long as the mosaicity is small. Therefore, experiments cannot be carried out with crystals of an intrinsic high mosaicity or to extremely high accumulated doses which increase the mosaicity as well (see Fig. 6). Whether the analyser crystal technique (Fig. 2) might be useful in the latter case has still to be investigated. (ii) The crystals have to be bathed in the beam; experiments with crystals larger than the beam diameter or with only partly illuminated crystals did not fit well into the general picture presented here. Therefore, it is expected that the situation of a partly illuminated protein crystal confined into a frozen liquid film should be even more complicated. In this case, d-spacing measurements might not be a suitable measure to quantitatively monitor radiation damage.

The small-molecule light-atom compounds investigated showed a linear increase of the lattice spacing with radiation dose within the range of the available flux densities. The rate of the lattice-spacing change is also linear with the flux density at least in the range that was available for these experiments. It was possible to separate a possible temperature-induced change in d-spacing from the one related to dose because of this linear behaviour. Within the accuracy of this method ($\sim$1–2 K) no significant increase in temperature could be observed up to a flux density of $\sim 5 \times 10^{12}$ photons s^{-1} mm^{-2}. It is certainly possible to design future experiments to be even more sensitive with respect to the accuracy for the determination of the temperature change. However, in the present case this seemed not to be necessary. The same holds for the time delay between switching the beam's intensity and the first d-spacing data point. This will be necessary for significant higher flux densities. It can be achieved by the technique using an analyser crystal since it provides very accurate d-spacing changes with a single scan. The predicted time for establishing an equilibrium temperature (Nicholson *et al.*, 2001) is well below 1 s. For this reason it will hardly be possible to track the temporal evolution of this process by the method presented here even if it should be possible to achieve a sufficiently high angular resolution. However it should be possible to obtain the first data point shortly after the temperature reaches equilibrium.

For practical reasons our investigations were mainly limited to one direction in reciprocal space. We have little evidence that other directions will behave fundamentally differently. However, since crystals are anisotropic the d-spacing change due to absorbed radiation dose has certainly to be described by a proper tensor. Whether this will provide new insights into these processes still needs to be investigated as well.

If one assumes that the rate-controlling process is the same at 100 K and *e.g.* at 20 K, cooling with a cold He-gas stream could significantly improve the lifetime of the crystal. However, many factors have to be taken into account for this case since the heat conductivity as well as the specific heat capacity is in general much smaller at extremely low temperatures. Whether the obtained results can easily be transferred to real protein crystals still has to be investigated in detail, since little is known about the difference in heat conductivity between the investigated organic small-molecule compounds and frozen protein crystals.

In order to retrieve the most diffracted intensity for a given radiation damage the optimum wavelength for organic light-atom compounds seems to be between 0.6 and 1.0 Å. This value will certainly shift to higher energies if a significant number of heavier atoms are present. However, if specific groups are preferred targets for the radiation damage, like the disulphide bonds in proteins (Weik *et al.*, 2000), the situation might look totally different. In these cases the very simple approach of using a single parameter to monitor radiation damage is certainly not enough to monitor the behaviour of the whole system.

The experimental dd/dt values normalized to the absorbed energy show little variance below 1.3 Å. However, there is a strong increase above that wavelength. It seems that qualitatively the photoelectrons in the lower energy range, which carry the most energy after an inelastic event, are producing more damage compared with at higher energies. Similar statements can be found elsewhere (Nave, 1995) based on empirical observations. Estimates based on inelastic electron-scattering cross sections from EEDL (Perkins *et al.*, 1991) reveal a mean free electron path length of about 140 Å and 370 Å for 8 keV and 24 keV electron energy, respectively, in light-atom small-molecule compounds. The mean energy loss per inelastic scattering event is about 40 eV and shows only a weak dependence on the energy of the incident electron. On average all scattering process do not change the direction of the incident electron significantly. Therefore, the energy of an absorbed high-energy (*e.g.* 24 keV) photon is spread

over a much larger volume as is the case for the corresponding number of photons of lower energy (*e.g.* of three 8 keV electrons). These results indicate that the closer neighbourhood of damage 'islands' causes more severe damage compared with those that are further apart. For a better understanding of this effect, more elaborate theoretical as well as experimental studies are needed.

References

Arndt, U. W. (1984). *J. Appl. Cryst.* **17**, 118–119.

Blake, C., Koenig, D., Mair, G., North, A., Philipps, D. & Sarma, V. (1965). *Nature (London)*, **206**, 757–761.

Bond, W. (1960). *Acta Cryst.* **13**, 814–818.

Burmeister, W. P. (2000). *Acta Cryst.* D**56**, 328–341.

Cullen, D. E., Hubbell, J. H. & Kissel, L. (1997). *EPDL*97*: the Evaluated Photon Data Library*, 1997 Version. University of California, LLNL, Livermore, CA 94550, USA.

Garman, E. & Schneider, T. (1997). *J. Appl. Cryst.* **30**, 211–237.

Gonzalez, A., Denny, R. & Nave, C. (1994). *Acta Cryst.* D**50**, 276–282.

Helliwell, J. R. (1992) *Macromolecular Crystallography with Synchrotron Radiation.* Cambridge University Press.

Hynes, R. & Le Page, Y. (1991). *J. Appl. Cryst.* **24**, 352–354.

Müller, R., Stojanoff, V., Siddons, P. & Weckert, E. (2002). To be published.

Nave, C. (1995). *Radiat. Phys. Chem.* **45**, 483–490.

Nicholson, J., Nave, C., Fayz, K., Fell, B. & Garman, E. (2001). *Nucl. Instrum. Methods A*, pp. 1380–1383.

Perkins, S., Cullen, D. & Seltzer, S. (1991). Technical Report UCRL-50400. Lawrence Livermore National Laboratory, Livermore, CA, USA.

Ramanadham, M., Sikka, S. & Chidambaran, R. (1972). *Acta Cryst.* B**28**, 3000–3005.

Ravelli, R. & McSweeney, S. (2000). *Structure*, **8**, 315–328.

Weckert, E. & Hümmer, K. (1997). *Acta Cryst.* A**53**, 108–143.

Weik, M., Ravelli, R., Kryger, G., McSweeney, S., Raves, M., Harel, M., Gros, P., Silman, I., Kroon, J. & Sussman, J. (2000). *Proc. Natl Acad. Sci. USA*, **97**, 623–628.

Weik, M., Ravelli, R., Silman, I., Sussmann, J., Gross, P. & Kroon, J. (2001). *Protein Sci.* 1953–1961.

Zellner, J. (1996). Diploma thesis, University of Karlsruhe, Germany.